Table-like magnetocaloric effect in $Gd_{56}Ni_{15}Al_{27}Zr_2$ alloy and its field independence feature

E. Agurgo Balfour,[1] Z. Ma,[1] H. Fu,[1,a)] R. L. Hadimani,[2,3] D. C. Jiles,[2,3] L. Wang,[1] Y. Luo,[1] and S. F. Wang[4,a)]

[1]*School of Physical Electronics, University of Electronic Science and Technology of China, Chengdu 610054, People's Republic of China*
[2]*Department of Electrical and Computer Engineering, Iowa State University, Ames, Iowa 50011, USA*
[3]*Ames Laboratory, U.S. Department of Energy, Ames, Iowa 50011, USA*
[4]*North Electronic Device Research Institute, Beijing 100141, People's Republic of China*

In order to obtain "table-like" magnetocaloric effect (MCE), multiple-phase $Gd_{56}Ni_{15}Al_{27}Zr_2$ alloy was prepared by arc-melting followed by suck-casting method. Powder x-ray diffraction and calorimetric measurements reveal that the sample contains both glassy and crystalline phases. The fraction of the glassy phase is about 62%, estimated from the heat enthalpy of the crystallization. The crystalline phases, Gd_2Al and $GdNiAl$ further broadened the relatively wider magnetic entropy change $(-\Delta S_M)$ peak of the amorphous phase, which resulted in the table-like MCE over a maximum temperature range of 52.5 K to 77.5 K. The plateau feature of the MCE was found to be nearly independent of the applied magnetic field from 3 T to 5 T. The maximum $-\Delta S_M$ value of the MCE platforms is 6.0 J/kg K under applied magnetic field change of 5 T. Below 3 T, the field independence of the table-like feature disappears. The relatively large constant values of $-\Delta S_M$ for the respective applied magnetic fields have promising applications in magnetic refrigeration using regenerative Ericsson cycle. © 2015 AIP Publishing LLC. [http://dx.doi.org/10.1063/1.4931765]

I. INTRODUCTION

The vapor compression/expansion refrigerator has today become an indispensable household appliance. However, there are global environmental concerns about its low efficiency and use of greenhouse gases.[1,2] A promising and efficient cooling process that does not use hazardous and ozone depleting gases is based on magnetocaloric effect (MCE). While the best conventional gas technology can achieve up to about 45% efficiency, magnetic prototypes are known to reach higher efficiency of 60% of the theoretical limit.[3] This improved performance has indirect impact on reduced CO_2 release.[4]

Magnetocaloric materials (MCMs) play a key role in the progress of this technology; hence, there is increased research on identifying MCMs that meet the requirements for high system output close to that of the Carnot cycle.[5] Ericsson cycle is one of the appropriate and practical thermodynamic cycles suitable for magnetic refrigeration above 15 K.[6,7] It requires that the magnetic entropy change $(-\Delta S_M)$ of the MCM remains constant over the working temperature range.[8] Such materials are said to exhibit "table-like" MCE and are characterized by the existence of suitably graded transition temperatures.[9] Unfortunately, this property is not commonly found in naturally occurring single phase magnetic materials but often achieved by design. For example, by pressing and sintering ferromagnetic materials with neighboring phase transitions or employing monolithic structural phase materials with successive magnetic phase

transitions such as in the $(Gd_{0.54}Er_{0.46})$ NiAl heat treated alloy.[10] In pressing and sintering, solid-state reactions between constituent materials and entropy generation in physical mixtures (due to temperature differences between neighboring particles) alter the expected temperature profile of $-\Delta S_M$ and reduce the overall efficiency of the thermodynamic cycle. Also, differences in the coefficient of thermal expansion (CTE) in sintered layers could potentially cause thermal stress that may lead to shattering of the material of lower CTE or result in the separation of the layers at the interface with time. As such, an ideal refrigerant suitable for Ericsson cycle should be a single bulk table-like MCM.

Several works on the broadening of $-\Delta S_M$ or on the improvement of refrigerant capacity (RC) have been reported in literature.[11,12] In particular, the flattening of $-\Delta S_M$ was observed over the temperature range of 20 K–300 K in the multi-phase $LuFe_2O_4$.[13] Unfortunately, because of its low $-\Delta S_M$ magnitude of approximately 1 J/kg K for a field change of 6.0 T its discovery was not appreciated. Fu *et al.* later reported table-like MCE in the multi-phase Gd-Co-Al alloy system containing both crystalline and amorphous phases and suggested that multi-phase alloys could be a useful means of obtaining table-like MCE.[14]

In this work, we study the magnetic and magnetocaloric properties of the multi-phase alloy $Gd_{56}Ni_{15}Al_{27}Zr_2$. We induce the formation of amorphous phase in the study alloy with the low content of Zr. Quaternary Gd-Ni-Al-Zr alloys were prepared using trace amounts of Zr for microalloying to obtain a multi-phase material with both crystalline and amorphous phases. The magnetic properties of the alloy and its component phases were analyzed by magnetic

a)Authors to whom correspondence should be addressed. Electronic addresses: fuhao@uestc.edu.cn and rockingsandstorm@163.com

measurements and its overall magnetocaloric performance was determined. Generally, MCE is dependent on the applied magnetic field.[15,16] In a material with table-like MCE, the nature and sensitivity of the field dependence of $-\Delta S_M$ of the components or phases often causes the disappearance of the platform under different applied fields. Interestingly, the constant $-\Delta S_M$ feature obtained in this alloy was found to be nearly independent of the field, in the range of 3 T to 5 T. We thus report table-like MCE and its uniqueness in the bulk multi-phase $Gd_{56}Ni_{15}Al_{27}Zr_2$ alloy.

II. EXPERIMENTAL

Gd metal of purity 99.2 wt. % and Ni, Al, and Zr metals all of purities 99.99 wt. % were used to prepare the $Gd_{56}Ni_{15}Al_{27}Zr_2$ and $Gd_{55}Ni_{17}Al_{26}Zr_2$ alloys under argon atmosphere at a chamber pressure of 1 atm in a water cooled WK-II arc furnace from Physcience Opto-Electronics. The ingots were repeatedly melted and then suck-casted in a copper mold to form 3 mm cylindrical rods. Powder x-ray diffraction (XRD) patterns were collected using a DX-2700 diffractometer operating at 40 kV and 30 mA with Cu K_α radiation for phase characterization. Step scanning mode with a step size of $0.02°$ and count time of 5 s/step was employed to obtain data with good signal-to-noise ratio. Calorimetric measurements were performed on a Setaram DSC131 calorimeter with a scanning rate of 20 K/min under nitrogen atmosphere. The magnetization measurements were performed on an MPMS XL-7 superconducting quantum interference device (SQUID) magnetometer, from Quantum Design, Inc.

III. RESULTS AND DISCUSSION

Fig. 1 shows the XRD pattern of the $Gd_{56}Ni_{15}Al_{27}Zr_2$ alloy. Sharp Bragg peaks can be seen with two broad peaks located at about $34°$ and $60°$. It suggests the coexistence of both crystalline and amorphous phases. The crystalline phases were determined to be Gd_2Al and GdNiAl, which are known to have the Co_2Si-type[17] and ZrNiAl-type[18] structures, respectively. The Bragg peaks of crystalline Gd_2Al and GdNiAl phases within $2\theta = 40°$ are indicated by asterisk and square (see Fig. 1), respectively. The inset of
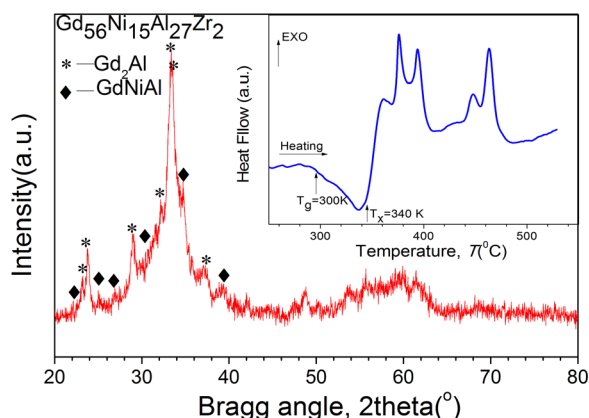
Fig. 1 shows the differential scanning calorimetry (DSC) trace of the title alloy. One glass transition near $300°C$ followed by several crystallization exothermic peaks above $340°C$ can be observed, confirming the presence of amorphous phase. The heat enthalpy of the crystallization reaction is measured to be 25.6 J/g. In comparison, that of $Gd_{55}Ni_{17}Al_{26}Zr_2$ (not shown) bulk metallic glass (BMG), which was used in the analysis of the magnetic properties of the title alloy is 41.3 J/g. Therefore, the phase fraction of the amorphous component was estimated at 62% (=25.6/41.3). The crystalline phases as observed by optical microscope (not shown) form in the center of the $Gd_{56}Ni_{15}Al_{27}Zr_2$ rod because of the slower cooling rate while the amorphous phase forms in the faster cooled outer.

The temperature dependence of magnetization for the $Gd_{56}Ni_{15}Al_{27}Zr_2$ alloy and that of its crystalline component phases under the applied magnetic field of 0.1 kOe is shown in Fig. 2. The magnetization was measured as the sample was cooled to low temperatures. The title alloy exhibits a broad ferromagnetic phase transition within 60–90 K with a Curie temperature of 70 K, determined from the minimum of the derivative of magnetization versus temperature (dM/dT) curve as shown in the inset of Fig. 2. To better understand the contribution of the amorphous phase to the phase transformation of our sample, a magnetization versus temperature (M-T) curve of $Gd_{55}Ni_{17}Al_{26}Zr_2$ BMG is also shown in Fig. 2. It is worth noting that glass forming ability is very sensitive to chemical concentration, and as a result, the $Gd_{55}Ni_{17}Al_{26}Zr_2$ alloy is wholly glassy structure while $Gd_{56}Ni_{15}Al_{27}Zr_2$ alloy, with 1 at. % difference in Ni and Al concentrations is BMG matrix composite. Both the BMG and the title alloy of 3 mm diameters were prepared under same conditions, such as the source and purity of raw materials, the chamber pressure, and the electric current. Therefore, the BMG is assumed to have similar properties (for example, glass transition, heat enthalpy of the crystallization reaction, and Curie temperature) to the glassy component of the title alloy. From the M-T curves, $Gd_{55}Ni_{17}Al_{26}Zr_2$ BMG shows ferromagnetic behavior and undergoes phase transition near 70 K. That of crystalline GdNiAl phase, as shown in Fig. 2, undergoes successive

FIG. 1. XRD pattern of $Gd_{56}Ni_{15}Al_{27}Zr_2$ alloy showing the Gd_2Al and GdNiAl peaks. Inset is the DSC curve of the sample.
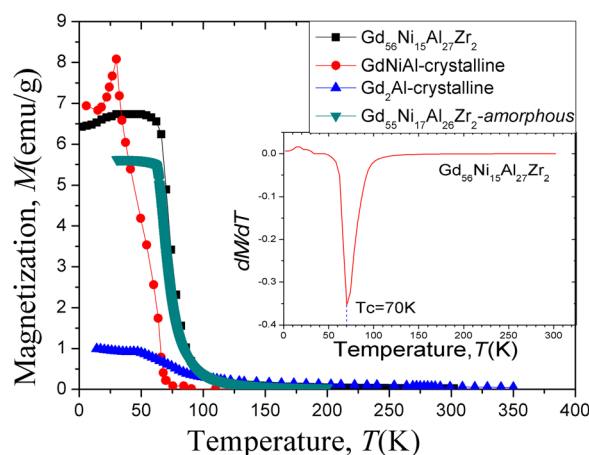

FIG. 2. Temperature dependence of magnetization for the alloy, its two crystalline component phases, and the BMG. The inset shows the derivative of magnetization versus temperature curve for the sample alloy.

phase transitions with the first occurring near 30 K. Its transition temperature, T_C is 67 K. The T_C of GdNiAl reported in literature ranges from 58 to 70 K.[19–21] Previous research[22] indicates that the substitution between Ni and Al can change the transition temperature of intermetallic phase GdNiAl. The higher the concentration of Ni in the phase, the higher is the transition temperature. Therefore, the GdNiAl phase in the title alloy may have higher concentration of Ni and possess similar transition temperature with the glassy phase. GdNiAl is also known to show negligible hysteresis (Ref. 18). Finally, the Gd_2Al phase undergoes two transitions near 50 K and about 270 K.[23] The transition near 50 K is from antiferromagnetism to paramagnetism. The high temperature transition near 270 K is from paramagnetism to ferromagnetism (Ref. 23). Considering the weak transition of Gd_2Al phase and its content in the alloy, its contribution to the phase transition for the title alloy cannot be distinguished from other component phases. Therefore, from the *M-T* curve, the broad ferromagnetic phase transition for the multi-phase structure alloy $Gd_{56}Ni_{15}Al_{27}Zr_2$ is attributable to the contribution of both the glassy phase and the crystalline GdNiAl.

The magnetization isotherms of $Gd_{56}Ni_{15}Al_{27}Zr_2$ alloy for applied fields between 0 and 50 kOe are shown in Fig. 3. When temperatures are higher than 110 K, the magnetization increases linearly with increasing applied field, indicating the alloy is paramagnetic. For the temperature range of 50 K to 90 K, the magnetization exhibits the characteristics of ferromagnetism for applied fields lower than 10 kOe. However, the magnetization increases linearly with the applied field from 10 kOe to 50 kOe. At temperatures lower than 40 K, delicate field-induced metamagnetic transitions can be observed when the applied field is above 20 kOe. For Gd_2Al phase, metamagnetic transition from antiferromagnetic to ferromagnetic (AFM-FM) induced by external magnetic field when temperature is lower than 40 K is observed as reported in literature (Ref. 23). The delicate field-induced metamagnetic transition is due to contribution of the Gd_2Al phase which is also confirmed by the XRD analysis. The maximum magnetization at 2 K for 50 kOe is 157 emu/g, i.e., 297.9 μ_B/f.u. or 5.3 μ_B/Gd, which is lower than that of the theoretical value of 7.0 μ_B/Gd.
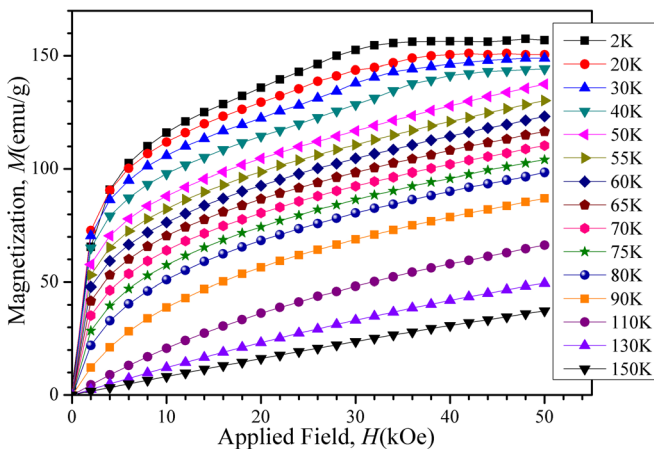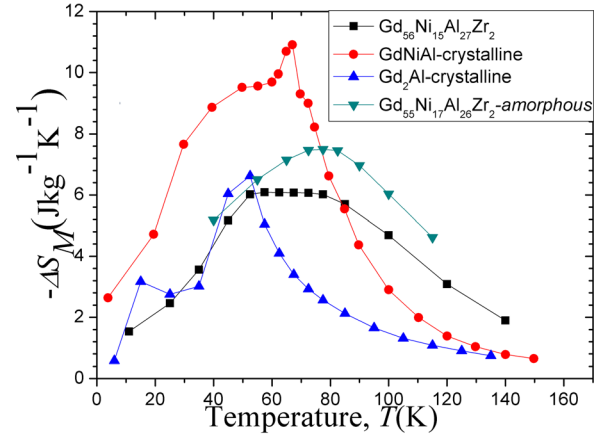

FIG. 4. Temperature dependence of $-\Delta S_M$ for the $Gd_{56}Ni_{15}Al_{27}Zr_2$ alloy showing table-like MCE and those of its component phases for $\Delta H = 50$ kOe.

It suggests that antiferromagnetic interaction exists in the alloy.

Fig. 4 shows the temperature dependence of the magnetic entropy change for the $Gd_{56}Ni_{15}Al_{27}Zr_2$ alloy at $\Delta H = 50$ kOe calculated from the magnetization isotherm measurements using Maxwell's relation.[24] The component crystalline phases of Gd_2Al, GdNiAl, and the full glassy alloy with a composition of $Gd_{55}Ni_{17}Al_{26}Zr_2$ are also shown in the figure. We note that the practical composition of the amorphous phase in $Gd_{56}Ni_{15}Al_{27}Zr_2$ is not exactly the same as $Gd_{55}Ni_{17}Al_{26}Zr_2$ but close to it. Table-like MCE was obtained in the parent multi-phase $Gd_{56}Ni_{15}Al_{27}Zr_2$ alloy, within the temperature range of 52.5 K to 77.5 K under an applied field of 5 T. In this temperature region of interest, Gd_2Al is paramagnetic and shows no hysteresis. The magnitudes of the magnetic entropy changes (MEC) of $Gd_{55}Ni_{17}Al_{26}Zr_2$ BMG at 72.5, 77.5, and 82.5 K are all 7.5 J/kg K. Thus, the resulting table-like MCE is attributed to further broadening of the MEC peak of the amorphous phase by crystalline GdNiAl and Gd_2Al under a suitable distribution of phase proportions and Curie temperatures. A similar effect has been reported in the study of $Gd_{60}Al_{10}Mn_{30}$.[25]

The obtained constant feature of $-\Delta S_M$ is nearly independent of the applied magnetic field as shown in Fig. 5.

FIG. 3. Magnetization isotherms of $Gd_{56}Ni_{15}Al_{27}Zr_2$ alloy at temperatures from 2 K to 150 K for $\Delta H = 50$ kOe.
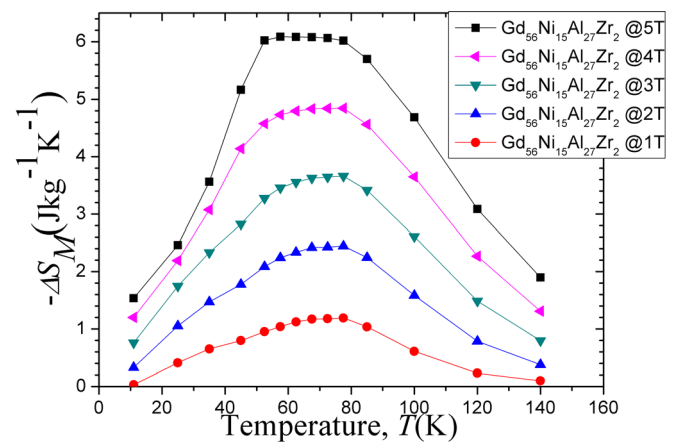

FIG. 5. Temperature dependence of magnetic entropy change of the $Gd_{56}Ni_{15}Al_{27}Zr_2$ sample alloy under different applied magnetic field changes.

TABLE I. Magnitudes and widths of $-\Delta S_M$ under given applied magnetic fields for different materials.

Material	Transition temperature (K)	Applied field (T)	$-\Delta S_M$ magnitude (J/kg K)	Width (K)	Reference
$Gd_{56}Ni_{15}Al_{27}Zr_2$	70	5	6.0	25	This work
$Gd_{52.5}Co_{16.5}Al_{31}$	$\sim$80	5	7.3	30	14
$Gd_{53}Co_{19}Al_{28}$	50–90	5	7.0	30	14
$[Fe_{87}Zr_6B_6Cu]_x$-$[Fe_{90}Zr_8B_2]_{1-x}$	240 and 300	5	2.4	80	26
Nd_2Fe_{17}	330	1.5	$\sim$1.0	20	27
$Fe_{78-x}Ce_xSi_4Nb_5B_{12}Cu$	281–465	5	2.0	80	28
$Fe_{88-x}Nd_xCr_8B_4$	322–350	5	3.2	40	29

The plateaus are satisfactorily flat with a maximum magnitude of 6.0 J/kg K for the applied field change of 5 T. Under the reduced fields of 4 T and 3 T, the magnitudes of the $-\Delta S_M$ platforms drop to 4.8 and 3.6 J/kg K, respectively. The width of the magnetic entropy change at 5 T is about 25 K (from 52.5 K to 77.5 K) and shrinks from the low temperature end towards high temperatures with decreasing magnetic field change. Thus, the effect of the applied magnetic field on the individual MECs of the component phases maintains the table-like feature of $-\Delta S_M$ but with reduced width and magnitude as the applied magnetic field change decreases. When the applied field is lower than 2 T, the table-like feature gradually disappears. Since field-induced transformation is suppressed below 2 T as already discussed above, the low field disappearance of the $-\Delta S_M$ platform could be ascribed to it.

The transition temperatures, the magnitude of the MEC platforms, as well as the width of the platforms of several materials are listed in Table I for comparison. The materials in Table I can be divided into two types. One is the rare earth based materials, and the other is the transition metal iron based materials. For the rare earth based materials, they have relatively lower transition temperatures and higher magnitude of $-\Delta S_M$ platforms. In our previous study, the magnitudes of the 5 T table-like platforms are 7.3 and 7.0 J/kg K for $Gd_{52.5}Co_{16.5}Al_{31}$ and $Gd_{53}Co_{19}Al_{28}$ alloys, respectively (Ref. 14). The decrease in the magnitude of the platform here is the result of relatively lower maximum MEC of the component phases, GdNiAl and glassy phase given by 11 and 7 J/kg K for $\Delta H = 50$ kOe, respectively. In comparison, MEC of the component phases in the Gd-Co-Al alloys, $GdCo_{0.74}Al_{1.26}$, Gd_2Co_2Al, and glassy phase are 11.4, 10.4, and 9.6 J/kg K for $\Delta H = 50$ kOe, respectively. However, the iron based materials possess higher transition temperatures and lower magnitudes of $-\Delta S_M$ platforms near their transition temperatures mainly due to the large heat capacity of the materials near room temperature. For instance, the table-like feature in $Fe_{78-x}Ce_xSi_4Nb_5B_{12}Cu$ multilayer and powder composites have transition temperatures above room temperature and maximum $-\Delta S_M$ values of 2.0 and 1.87 J/kg K, respectively, under the applied field change of 5 T.[28] In the multilayer composite $Fe_{88-x}Nd_xCr_8B_4$, the magnitude of the platform is approximately 3.2 J/kg K for a field change of 5 T.[29]

Though the magnitude of the table-like MCE of the $Gd_{56}Ni_{15}Al_{27}Zr_2$ alloy is relatively lower than those of non-table-like model MCMs used in near liquid nitrogen temperature applications, such as $DyAl_2$ with second-order phase transition and Dy_5Si_3Ge with first-order transition,[30] it is comparatively large amongst other table-like MCMs and suitable for efficient magnetic refrigeration applications at low temperatures using regenerative Ericsson cycle.

IV. CONCLUSIONS

The quaternary $Gd_{56}Ni_{15}Al_{27}Zr_2$ alloy synthesized by suck-casting method possesses composite structure with both crystalline and the amorphous phases. The crystalline phases are Gd_2Al and GdNiAl determined by powder x-ray analysis. The glassy phase confirmed by calorimetric measurements has a phase fraction of about 62% estimated by its heat enthalpy in comparison with the full glassy alloy. The study alloy shows a broad phase transition from 60 K to 90 K in the M-T curve and exhibits table-like MCE. The magnitude and the width of the MEC platform are 6.0 J/kg K and 25 K for $\Delta H = 50$ kOe, respectively. The alloy's $-\Delta S_M$ platform exhibits field independent feature from 3 T to 5 T. It provides a single MCM with table-like MCE for Ericsson cycle applications under different magnetic fields.

ACKNOWLEDGMENTS

[1]V. K. Pecharsky and K. A. Gschneidner, Jr., Appl. Phys. Lett. **70**, 3299 (1997).
[2]M. Balli, D. Fruchart, D. Gignoux, E. K. Hlil, S. Miraglia, and P. Wolfers, J. Alloys Compd. **442**, 129 (2007).
[3]C. Zimm, A. Jastrab, A. Sternberg, V. Pecharsky, K. Gschneidner, Jr., M. Osborne, and I. Anderson, Adv. Cryog. Eng. **43**, 1759 (1998).
[4]E. Bruck, J. Phys. D: Appl. Phys. **38**, R381 (2005).
[5]W. Dai, J. Appl. Phys. **71**, 5272 (1992).
[6]T. Hashimoto and T. Kuzuhara, J. Appl. Phys. **62**, 3873 (1987).
[7]A. G. Diguet, G. Lin, and J. Chen, Int. J. Refrig. **36**, 958 (2013).
[8]A. Smaili and R. Chahine, J. Appl. Phys. **81**, 824 (1997).
[9]J. Liu, J. D. Moore, K. P. Skokov, M. Krautz, K. Lowe, A. Barcza, M. Katter, and O. Gutfleisch, Scr. Mater. **67**, 584 (2012).
[10]H. Takeya, V. K. Pecharsky, K. A. Gschneidner, and J. O. Moorman, Appl. Phys. Lett. **64**, 2739 (1994).
[11]C. F. Sánchez-Valdés, P. J. Ibarra-Gaytán, J. L. Sánchez Llamazares, M. Ávalos-Borja, P. Álvarez-Alonso, P. Gorria, and J. A. Blanco, Appl. Phys. Lett. **104**, 212401 (2014).
[12]R. Caballero-Flores, V. Franco, A. Conde, K. E. Knipling, and M. A. Willard, Appl. Phys. Lett. **98**, 102505 (2011).
[13]M. H. Phan, N. A. Frey, M. Angst, J. deGroot, B. C. Sales, D. G. Mandrus, and H. Srikanth, Solid State Commun. **150**, 341 (2010).
[14]H. Fu, Z. Ma, X. J. Zhang, D. H. Wang, B. H. Teng, and E. A. Balfour, Appl. Phys. Lett. **104**, 072401 (2014).

[15]V. Franco, J. S. Blázquez, and A. Conde, Appl. Phys. Lett. **89**, 222512 (2006).

[16]V. Franco, A. Conde, V. K. Percharsky, and K. A. Gschneidner, Jr., Europhys. Lett. **79**, 47009 (2007).

[17]X. G. Li, M. Sato, S. Takahashi, K. Aoki, and T. Masumoto, J. Magn. Magn. Mater. **212**, 145 (2000).

[18]L. Si, J. Ding, Y. Li, B. Yao, and H. Tan, Appl. Phys. A **75**, 535 (2002).

[19]K. H. J. Buschow, J. Less-Common Met. **39**, 185 (1975).

[20]J. Jarosz, E. Talik, T. Mydlarz, J. Kusz, H. Bohm, and A. Winiarski, J. Magn. Magn. Mater. **208**, 169 (2000).

[21]B. J. Korte, V. K. Pecharsky, and K. A. Gschneidner, J. Appl. Phys. **84**, 5677 (1998).

[22]B. Leon and W. E. Wallace, J. Less-Common Met. **22**, 1 (1970).

[23]P. Kumar, K. G. Suresh, and A. K. Nigam, J. Phys. D: Appl. Phys. **41**, 105007 (2008).

[24]V. K. Pecharsky and K. A. Gschneidner, Jr., Phys. Rev. Lett. **78**, 4494 (1997).

[25]S. Gorsse, B. Chevalier, and G. Orveillon, Appl. Phys. Lett. **92**, 122501 (2008).

[26]P. Álvarez, J. L. Sánchez Llamazares, P. Gorria, and J. A. Blanco, Appl. Phys. Lett. **99**, 232501 (2011).

[27]P. Alvarez-Alonso, J. L. Sánchez Llamazares, C. F. Sánchez-Valdés, G. J. Cuello, V. Franco, P. Gorria, and J. A. Blanco, J. App. Phys. **115**, 17A929 (2014).

[28]H. C. Tian, X. C. Zhong, Z. W. Liu, Z. G. Zheng, and J. X. Min, Mater. Lett. **138**, 64 (2015).

[29]J. W. Lai, Z. G. Zheng, X. C. Zhong, V. Franco, R. Montemayor, Z. W. Liu, and D. C. Zeng, J. Magn. Magn. Mater. **390**, 87 (2015).

[30]K. A. Gschneidner, Jr., V. K. Pecharsky, and A. O. Tsokol, Rep. Prog. Phys. **68**, 1479 (2005).